Proceedings of ERAD (2002): 155–160 © Copernicus GmbH 2002

ERAD 2002

Dynamic properties of clouds and dynamic/microphysical interactions from 94 Ghz cloud radar and lidar

A. Protat, C. Tinel, and J. Testud

CETP/UVSQ/CNRS, 10-12 Avenue de l'Europe, 78140 Vélizy, France

1 Introduction

The knowledge of the cloud properties has been recently identified as a mandatory step to reach if the operational weather and climate change forecasts are to be improved. In the framework of the future space missions devoted to the monitoring of the microphysical, radiative, and dynamic properties of clouds at global scale using cloud radar and lidar combination (CLOUDSAT/CALIPSO as part of the "Afternoon Train", NASA/CNES, and Earth-CARE, ESA), there is a need for ground-based and airborne validation of the radar/lidar measurements and products from these space missions.

The French RALI project addresses these issues through the development of a dual-beam Doppler cloud radar (RASTA, Radar Aéroporté et Sol de Télédétection des propriétés nuAgeuses, briefly described in Sect. 2 and a dual wavelength backscatter lidar (LEANDRE 1). The synergy between the two instruments is such that in moderately thick clouds the liquid/ice water content LWC/IWC and effective radius r_e of droplets/crystals can be retrieved from these two measurements (see Tinel et al. in the present proceedings). In this paper we primarily focus on the retrieval of the dynamics from the dual-beam cloud radar only. Among the dynamic properties of clouds two important aspects are addressed in the present paper: the retrieval of the along-track horizontal and vertical wind components, and the retrieval of the terminal fall velocity of the hydrometeors Vt. Knowledge of water drop and ice crystal terminal velocities is indeed particularly important for an adequate representation of particle sedimentation in operational forecast and climate models. For this purpose a method is proposed in Sect. 3 which extracts statistical relationships between Vt and radar reflectivity Z from the dual-beam Doppler measurements of the RASTA cloud radar. In Sect. 4, we report on results obtained with this method in a nimbostratus case sampled on 13 March 2001 in the Paris area during the CARL2001 campaign. It appears however that these relationships cannot be easily handled in large-scale models, since radar reflectivity is not the most tractable variable for these models. Therefore, a radar-lidar algorithm (Tinel et al., 2002) is used in Sect. 5 to recover the microphysical and radiative properties of clouds (IWC and r_e). Tractable statistical relationships to be used in models are finally developed between Vt and IWC/Vt and r_e.

Correspondence to: A. Protat (Alain.Protat@cetp.ipsl.fr)

2 The RASTA cloud radar

The RASTA cloud radar has been developed at CETP. It is a 95 GHz pulsed radar, 1.8 kW peak power, with a range resolution of 60 m (tunable), and a PRF of 25 kHz.

It is implemented in an airborne version and a ground-based version. The airborne version of RASTA is a dual-beam radar (antennas are 30.5 cm horn lens, 0.7° beamwidth, with a 47 dB gain), with a nadir-pointing beam, and a beam pointing 40° fore in the direction of the aircraft heading. It is installed on the Institut Géographique National Fokker 27 aircraft (ARAT) since September 2000. The airborne version has been validated during the CARL2000 campaign, which was held in November 2000 in Brest, France. Its sensitivity was found to be -23 dBZ at 1 km range, but this sensitivity is being presently improved (-27 dBZ expected). In the next two years, RASTA will be modified to fit in a wing pod. This will allow an easier deployment on several aircraft for future campaigns.

The ground-based version of RASTA has been implemented in a van, with a single 1.22 m Cassegrain antenna pointing vertically. The first tests indicate that the sensitivity of the ground-based version after 1 s integration will be around -50 dBZ at 1 km. This radar will collect systematic observations from the SIRTA (an experimental site fully-instrumented for cloud, aerosol, and water vapor studies in Palaiseau, France) in the period 2002–2004 in the framework of the EC project CloudNet (see http://www.met.rdg.ac.uk/radar/cloudnet/ for further details about the scientific objectives of CloudNet).

3 Retrieval of dynamic properties from the airborne version of the cloud radar RASTA

The method to recover the dynamic properties of clouds relies upon the combination of the 40° fore and nadir beams of the dual-beam cloud radar. For each beam direction (azimuth α, elevation el, see Fig. 1) the radial velocity Vr at a given range r may be expressed as a function of the horizontal wind component parallel to the aircraft heading ($V_{\|}$, positive in the direction of the heading) and of the sum ($Vt + w$) of terminal fall speed of the hydrometeors and vertical air velocity (velocity is positive upward):

$$Vr(r) = V_{\|}(r)\delta\cos(el) + (Vt(r) + w(r))\sin(el) \quad (1)$$

where $\delta = +1$ when the antenna points in the heading direction, $\delta = -1$ when it points in the opposite direction (this latter configuration happens for the nadir beam when the aircraft nose points downward, i.e. the pitch is <0).

First the radial velocities and radar pointing angles are corrected for several effects: the pointing angles are corrected for the aircraft pitch, roll, and drift following the procedure described in Lee et al. (1994); the projection of aircraft ground speed along the beams is removed from the Doppler measurements, and the radial velocities are unfolded using the in-situ wind sensor as a reference for the first gate, a gate-to-gate correction is then applied for the next gates, allowing a maximum wind shear from one gate to the next (for further details, see Protat et al., 1997); the gates contaminated by ground echoes and below the ground are removed. Finally, radar beams for which the absolute value of the aircraft roll is greater than 1° are removed, in order to minimize errors due to the projection of the cross-track horizontal wind component onto the radar beams, which is neglected in the method described hereafter. It is important to mention that the flight plans were designed in such a way that we flew along the flight-level wind. If a cross-track component of 5 ms^{-1} is considered, the projection onto the radar beams would lead to a 0.08 ms^{-1} peak error for a 1° roll. Larger errors can be expected in cases of strong vertical wind shear.

In a second step the data from each antenna are reorganized into a two-dimensional Cartesian grid. A trade-off for the grid size has been searched, in order to keep the best resolution for the retrieved two-dimensional field on the one hand, but to filter out the measurement noise and errors introduced by the roll angle on the other hand. A grid mesh of 300 m horizontally and 100 m vertically is used in what follows. Let us recall that due to aircraft motion, the horizontal resolution of our measurements is around 20 m horizontally (for a typical ground speed of 120 ms^{-1}), and 60 m along the beams. This leads to an average of 30 points at most in each grid. The mean roll angle is computed in order to monitor the expected accuracy of the retrieved two-dimensional field in each grid.

The method for retrieval of the two wind components $V_{\|}$ and ($Vt + w$) simply consists in solving for each grid the set of two equations derived from Eq. (1), which leads to the following equations:

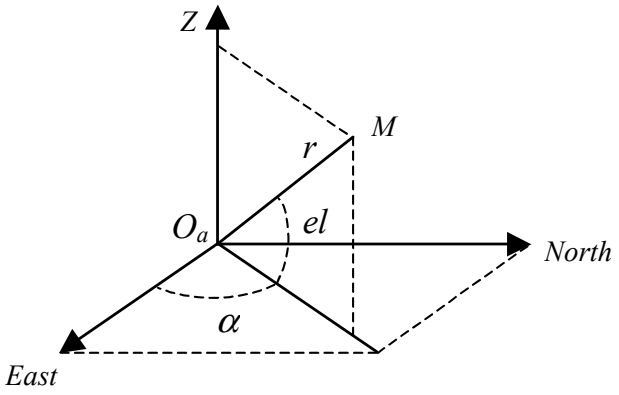

Fig. 1. Definition of the azimuth α, elevation el, and range r in the earth-relative coordinate system. The radar is located at its origin O_a.

$$V_{\|} = \frac{V_1\sin(el2) - V_2\sin(el1)}{\cos(el2)\sin(el1) - \delta\cos(el1)\sin(el2)} \quad (2)$$

$$Vt + w = \frac{V_2\delta\cos(el1) - V_1\cos(el2)}{\cos(el2)\sin(el1) - \delta\cos(el1)\sin(el2)} \quad (3)$$

where subscripts 1 and 2 refer to the nadir and 40° fore measurements, respectively.

Up to here, the terminal fall velocity and vertical wind component are not separated. In order to estimate the terminal fall velocity, a statistical approach is proposed in what follows, as already discussed for frontal cyclones in Protat et al. (2000, 2002). Within weakly-precipitating clouds, the vertical air motions are generally small, even at small scales of motion, as opposed to the case of convective systems. In any case, however, the vertical air motions are not negligible with respect to the terminal fall speed, but if the procedure described previously is applied to a long time span (a whole aircraft mission, for instance), then *the mean vertical air motions should vanish with respect to the mean terminal fall speed*, which is much less fluctuating. A statistical power-law relationship between the terminal fall speed and radar reflectivity may therefore be derived from this statistical approach. This hypothesis has been recently validated in the case of frontal cyclones sampled during FASTEX (Protat et al., 2002). A more thorough validation of this assumption will be performed in a near future using high-resolution numerical simulations of cirrus clouds.

4 The 13 March 2001 nimbostratus (CARL2001)

An ESA funded airborne campaign named CARL 2001 was held in Brétigny-sur-Orge, France. Two aircraft were involved in order to document the microphysical, radiative and dynamic properties of clouds: the ARAT aircraft, carrying

the RASTA cloud radar and the LEANDRE I backscatter lidar, and the Météo-France MERLIN-IV aircraft carrying in-situ microphysical sensors for in-situ validation. Owing to the maximum flight level of the ARAT (5.5 km), the priority meteorological targets were mixed-phase or ice midlevel clouds and stratocumuli. The scientific objectives of this experiment were to derive from the radar-lidar observations the macrophysical (bottom and top of the cloud, vertical structure ...), microphysical (ice/liquid water content), radiative (r_e), and dynamic properties of clouds, in order to investigate the interaction between these processes, and in particular the dynamic/microphysical interactions.

Six Intensive Observing Periods (IOPs) have been conducted successfully, allowing different types of clouds to be investigated (altocumulus, cumulus congestus, nimbostratus, small cumuli, mixed-phase altocumulus), but only three IOPs included both the radar-lidar observations and the in-situ microphysics for validation. Among these three cases, the nimbostratus has been selected to evaluate the performances of the method described in the previous section, since it includes both liquid phase and ice phase precipitation. Figure 2 shows the flight track of the two aircraft, with the ARAT flight-level horizontal wind. It is observed on this figure that we flew almost parallel to the wind most of the time during the straight-line patterns, which is a favourable configuration for the method.

The first step of the retrieval is to recover the two particle velocity components $V_{\|}$ and $(Vt + w)$ using Eqs. (2) and (3). These wind components are shown as arrows on the vertical cross-section of Fig. 3 with the radar reflectivity (contours). The reflectivity field shows the typical feature of stratiform-like precipitation, with a well-defined bright-band at around 1.3 km altitude, indicative of the layer where ice crystals melt. The $(Vt + w)$ field shows the expected dynamic pattern, with velocities (modulated by the vertical air motion) of around -4 to -5 ms^{-1} in liquid phase (below the melting layer), -1 to $+0.2$ ms^{-1} in ice phase. On the upper-right part of the figure slightly larger negative values are retrieved in the lower part of the ice cloud and smaller negative values in the upper part of the ice cloud. This is likely indicative of either the presence of smaller ice crystals (thus falling at a smaller terminal fall speed) or larger upward air motions in the upper part of the ice cloud. Also, in this part of the cloud $(Vt+w)$ ranges from -0.4 to 0.2 ms^{-1}. After a careful inspection, it is found that these positive values of $(Vt + w)$ are correlated with the strongest small-scale reflectivity structures within this part of the cloud (not shown). In these small regions, the upward motions are sufficient to compensate for the sedimentation of precipitation and then lead to an enhancement of ice crystal growth.

The second step is to derive statistical relationships between $(Vt + w)$ and the radar reflectivity Z. Terminal fall velocity and reflectivity are integral parameters of the particle size distribution (PSD). Ulbrich (1983) for a Gamma-type PSD, and Testud et al. (2001) for a normalized PSD, established that the relationships between integral parameters were represented by power-law relationships. The

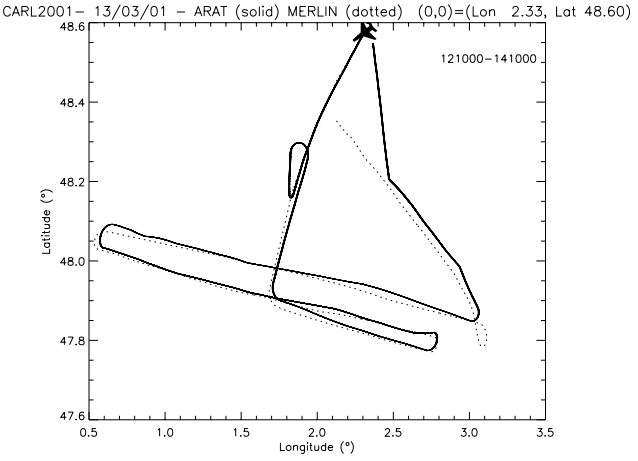

Fig. 2. Flight track of the ARAT (solid) / Merlin IV (dotted) on 13 March 2001 during the CARL2001 campaign. Arrows are the ARAT flight-level horizontal wind components every 30 s.

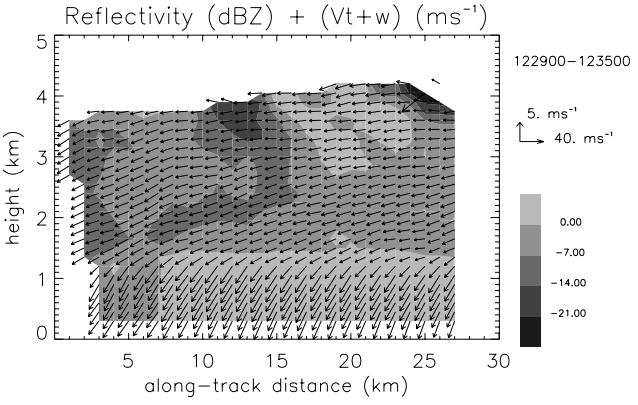

Fig. 3. Vertical cross section of reflectivity (contours) and 2D particle velocity (including fall speed) for the time span 12:29:00–12:35:00 UTC on 13 March 2001. Only one arrow out of three is drawn.

method proposed in this paper consists of estimating statistical power-law relationships $Vt = a\,Z^b$ between terminal fall speed and radar reflectivity by fitting the individual estimates of $(Vt + w)$ and Z, with caution exercised in order to process a time span long enough to make the mean vertical air velocity vanish with respect to the mean Vt. In order to separate the liquid and ice phases, we derive an estimate of the 0°C isotherm altitude using the temperature measurements taken from the two soundings performed when taking off and landing. Another indirect way to estimate the 0°C isotherm altitude is to look at the height of the radar "bright band" (radar signature of the melting layer) in the vertical cross-sections of radar reflectivity. The 0°C isotherm is located just above the bright band. Figure 4a shows the statistical relationships obtained in ice phase by processing the whole 13 March 2001 flight (from 12:15 to 13:50 UTC). In order to allow future comparisons with microphysical in-situ relationships, a density correction factor $f(z) = (\rho/\rho_0)^{0.4}$

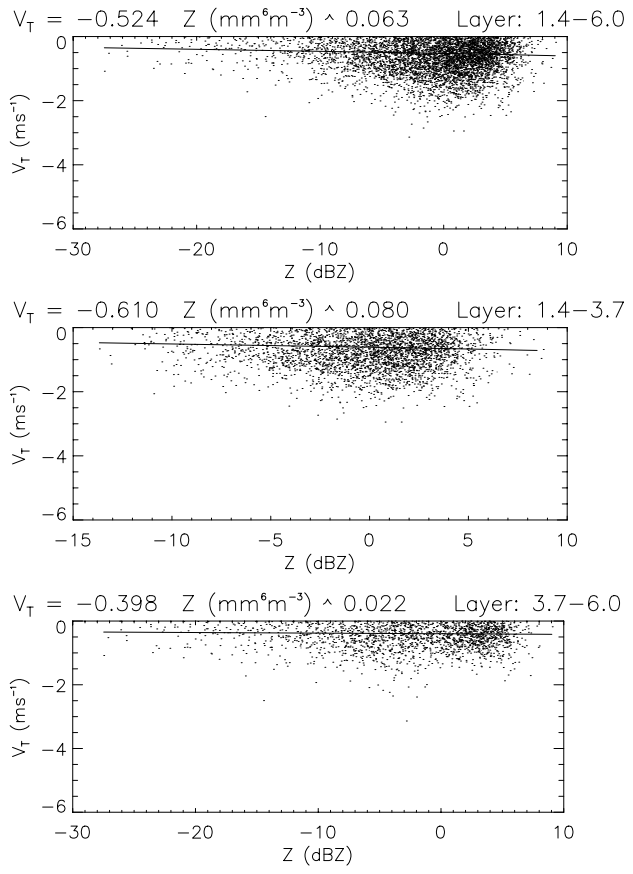

Fig. 4. $Vt - Z$ relationships in ice phase: (a) for the whole ice cloud, (b) for the lower part of the ice cloud (from 1.4 to 3.7 km height), and (c) for the upper part of the ice cloud (from 3.7 to 6 km). Also given are the coefficients of relations (solid curves) on top of each panel.

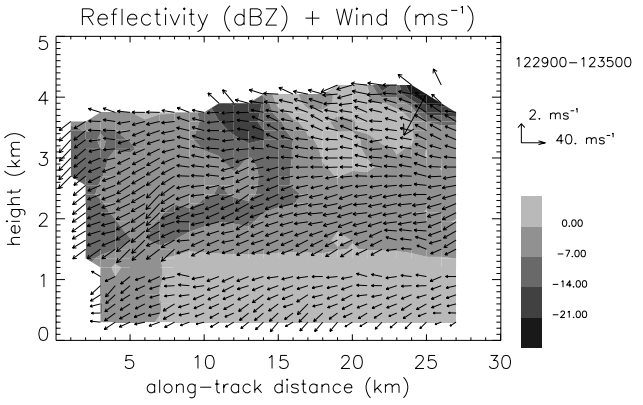

Fig. 5. Vertical cross section of reflectivity (contours) and 2D wind vectors (fall speed subtracted) for the time span 12:29:00–12:35:00 UTC on 13 March 2001. Only one arrow out of three is drawn.

has been applied to each $(Vt + w)$ estimate (Foote and Du Toit, 1969).

The statistical relationship estimated in ice phase (Fig. 4a) shows that the terminal fall velocity increases with reflectivity, as expected, with a value of -0.52 ms^{-1} for a 0 dBZ reflectivity. These values appear reasonable for ice crystal fall speeds. The relatively large scatter around the fitted curve is attributed to the contribution of the vertical air motions for each estimate of the terminal fall velocity. It must be noted that when processing the whole volume of ice, it is implicitly assumed that there is a single ice particle type, which is probably wrong most of the time. In order to evaluate the degree to which the ice type changes with height within this nimbostratus cloud, we separate in what follows the volume of ice into two sectors: the lower part (from 1.4 to 3.7 km) and the upper part (from 3.7 to 6 km) of the ice cloud. Then, the statistical relationships are computed for each sector. It is obtained that larger (smaller) terminal velocities are found in the lower (upper) part of the ice cloud (Fig. 4b and c). This is consistent with the presence of larger (smaller) ice crystals in the lower (upper) part of the cloud, which likely reflects the growth of the ice crystals through aggregation while ice crystals fall, as is generally encountered in the literature (e.g. Marecal et al., 1993). This result indicates that further studies are needed in order to take into account the variability of the statistical relationships with height.

The relationship obtained in liquid phase (not shown) are comparable to the relationships obtained for frontal cyclones by Protat et al. (2002). Nevertheless, the radar reflectivity in rain is not corrected for attenuation yet. Therefore the statistical $Vt-Z$ relationship in rain may be significantly biased in the present case. Work is under progress to correct the radar attenuation by taking advantage of the two different optical paths travelled by the two radar beams within the same water cloud.

The last step of the retrieval of the dynamic properties consists in subtracting terminal fall velocity (using the radar reflectivity field and the statistical relationships) from the $(Vt + w)$ field in order to access the 2D wind field. The 2D wind field corresponding to the vertical cross-section of Fig. 3 is shown in Fig. 5. Interesting features are recovered. It is seen that maximum upward motions of around 0.8 ms^{-1} are retrieved in the area where reflectivities are strongest (upper-right part of Fig. 5). In the liquid water part of the cloud, slightly downward motions dominate, with however slight small-scale updrafts in some parts, which is typical of mean vertical wind profiles in stratiform-like precipitation. It must be recalled however that attenuation is not corrected yet in the liquid water layer, which biases the estimate of Vt (and in turn the estimate of w) in the present case.

5 Derivation of relationships for large-scale models

In this section the documentation of the dynamics is combined with the microphysical and radiative properties derived from the radar-lidar observations (Tinel et al., 2002) in order to develop statistical relationships useful to large-scale models. The $Vt - Z$ relationships are probably not the most relevant in this respect, since reflectivity is not a variable readily

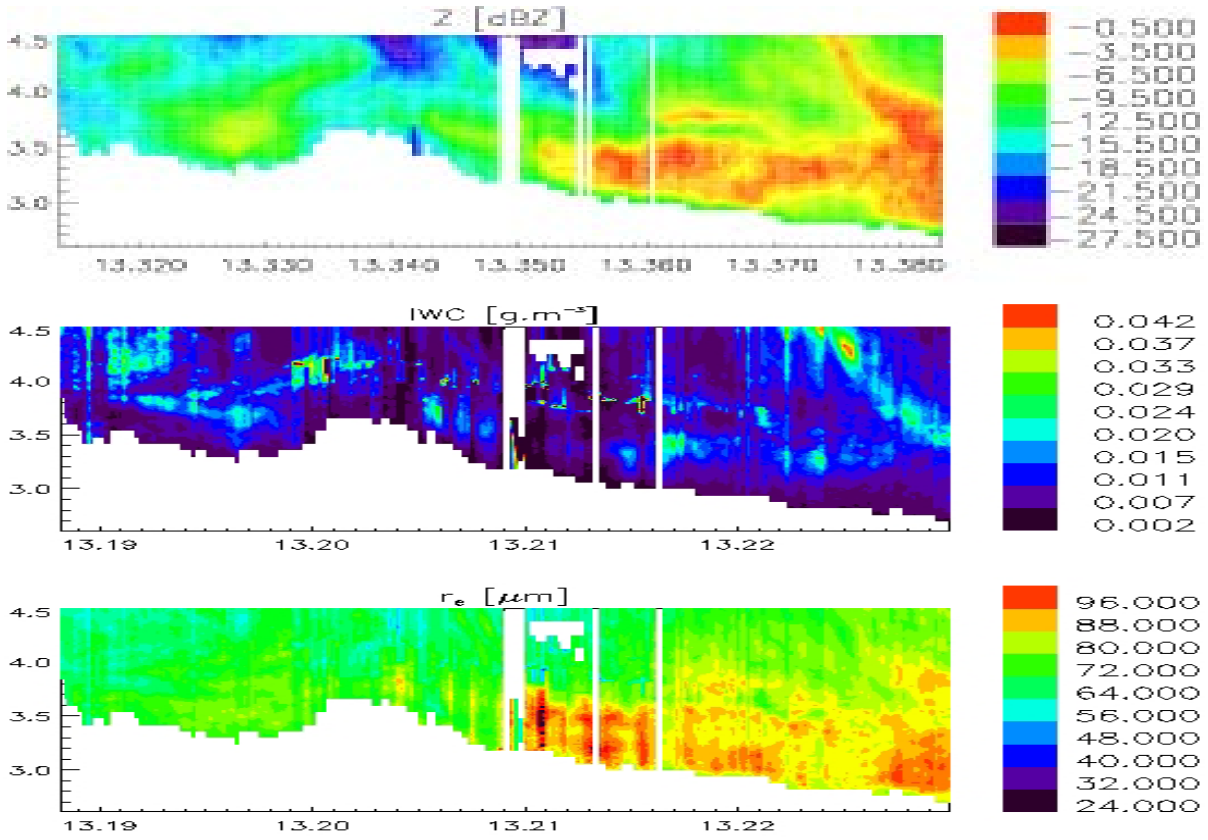

Fig. 6. Vertical cross-section of (a) measured radar reflectivity, and retrieved (b) ice water content, (c) effective radius using the radar-lidar algorithm of Tinel et al. (2002) in an altocumulus sampled on 10 November 2000 during the CARL2000 campaign.

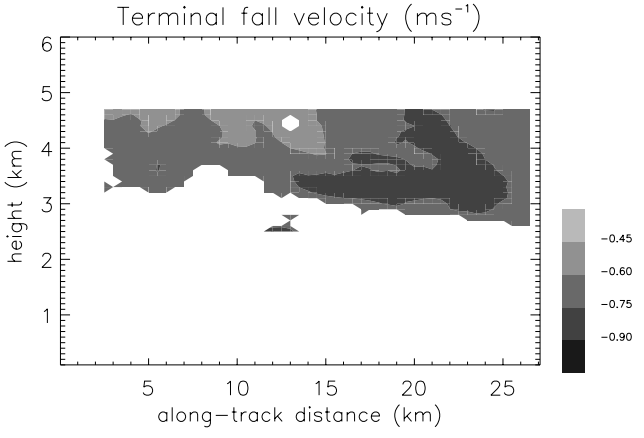

Fig. 7. Same as Fig. 6, except for the terminal fall velocity retrieved using the method described in the present paper.

available in a large-scale model (although it could be computed), while ice water content and effective radius are. A case from the CARL2000 campaign (same airborne setup as in CARL2001, see Sect. 4) is used to illustrate the capabilities of such an approach. The 10 November 2000 case is an altocumulus sampled from above by the dual-beam RASTA cloud radar and the nadir-looking 532 nm backscatter lidar LEANDRE. The retrieval of IWC and r_e obtained using the radar-lidar algorithm of Tinel et al. (2002) is shown in Fig. 6 in a 2D vertical cross-section. The retrieved values have been validated using the in-cloud sensor observations onboard the MERLIN IV aircraft. Within the same cloud, the statistical relationship between Vt and Z has been derived from the dual-beam Doppler observations of the cloud radar, and the radar reflectivity has been translated into terminal fall velocity in the 2D vertical cross-section of Fig. 6 (Fig. 7). Values of Vt ranging from -0.9 to -0.4 ms^{-1} are retrieved within the cloud. Then, using the results from Figs. 6 and 7, Vt can be plotted against IWC (Fig. 8a) and r_e (Fig. 8b) in order to develop statistical relationships between these quantities for this altocumulus case. This type of (preliminary) relationships are readily useful to large-scale models, since generally Vt is diagnosed from the particle size or IWC. It is seen though in Fig. 8 that some problems still need to be addressed. Indeed, two types of scatter points are observed on Fig. 8a, although a satisfying general trend is observed. Further studies show that the two distinct scatters are due to contributions at different heights. The scatter points with smaller fall speeds are located in the upper part of the cloud, while the scatter points with larger fall speeds are located in

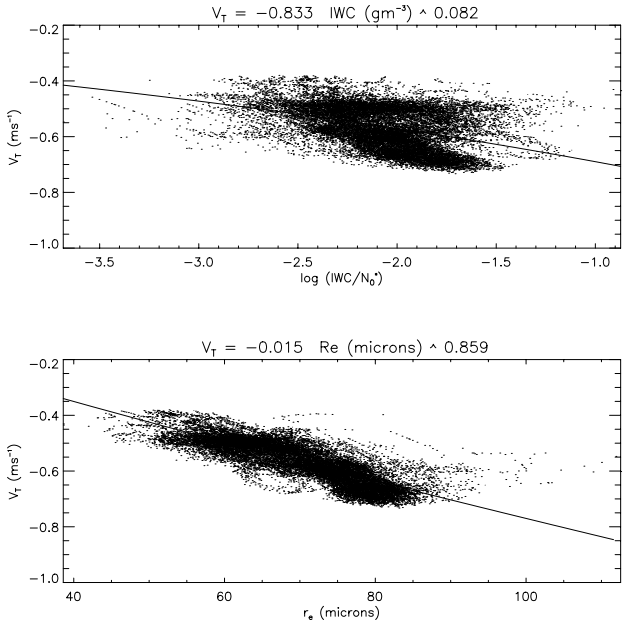

Fig. 8. Statistical relationships between (a) Vt and ice water content, (b) Vt and effective radius for the 10 Nov. 2000 altocumulus case (CARL2000).

the lower part of the cloud (not shown). In a near future, these scatters will be separated using either height or other criteria (such as temperature, lidar depolarisation ratio) in order to obtain more trustable relationships.

6 Future directions

In this paper, the dynamic properties of clouds are investigated using data from a dual-beam cloud radar, and statistical relationships between dynamic, microphysical and radiative quantities are developed. Remaining methodological tasks are (i) to correct the radar reflectivity for attenuation in liquid phase, (ii) to validate the main assumption carried out in the retrieval of the $Vt-Z$ statistical relationships, stating that for a long time span the mean vertical air motions should vanish with respect to the mean terminal fall speed, and (iii) to remove the super-cooled water layer from the scatter. Then, the description of the dynamics will be combined with the microphysical properties derived from the radar-lidar observations in order to investigate the interaction between the microphysics and dynamic processes.

Acknowledgement. This work is supported by the CloudNet European programme under contract EVK2 – CT2000 – 00065.

References

Foote, G. B., and P. S. Du Toit, 1969: Terminal velocity of raindrops aloft. J. Appl. Meteor., 8, 249-253.

Lee, W.-C., P. Dodge, F. D. Marks, and P. H. Hildebrand, 1994: Mapping of airborne Doppler radar data. J. Atmos. Oceanic Technol., 11, 572-578.

Marécal, V., D. Hauser, and F. Roux, 1993: The NCFR observed on 12-13 January 1988 during the MFDP/FRONTS87 Experiment. Part II: Microphysics. J. Atmos. Sci., 50, 975-998.

Protat, A., Y. Lematre, and D. Bouniol, 2002: Terminal fall velocity and the FASTEX cyclones, Submitted to the Quart. J. Roy. Meteor. Soc.

Protat, A., Y. Lematre, D. Bouniol, and R. A. Black, 2000: Microphysical observations during FASTEX from airborne doppler radar and in-situ measurements. Phys. Chem. Earth (B), 25, 1097-1102.

Protat, A., Y. Lematre, and G. Scialom, 1997: Retrieval of kinematic fields using a single-beam airborne Doppler radar performing circular trajectories. JAOT, 14, 769-791.

Testud, J., S. Oury, R. A. Black, P. Amayenc, X-K Dou, 2001: The Concept of "Normalized" Distribution to Describe Raindrop Spectra: A Tool for Cloud Physics and Cloud Remote Sensing. J. Appl. Meteor., 40 (6), 1118-1140.

Tinel, C., J. Testud, A. Protat, and J. Pelon, 2002: Combined radar and lidar observations for the retrieval of radiative and microphysical properties in ice clouds. Preprints, 11th Conference on Cloud Physics, AMS, Ogden, UT, USA, 3-7 June 2002.

Ulbrich, C. W., 1983: Natural variations in the analytical form of the drop size distribution. J. Clim. Appl. Meteor., 22, 1764-1775.